Author Manuscript

Author Manuscript

Author Manuscript

Author Manuscript

HHS Public Access

Author manuscript

Curr Eye Res. Author manuscript; available in PMC 2021 February 01.

Published in final edited form as:

Curr Eye Res. 2020 February ; 45(2): 162–172. doi:10.1080/02713683.2019.1662058.

Formation of cholesterol bilayer domains precedes formation of cholesterol crystals in membranes made of the major phospholipids of human eye lens fiber cell plasma membranes

Laxman Mainali[a,⊥], **Marta Pasenkiewicz-Gierula**[b], **Witold K. Subczynski**[a,*]

[a]Department of Biophysics, Medical College of Wisconsin, Milwaukee, Wisconsin 53226, USA
[b]Department of Computational Biophysics and Bioinformatics, Jagiellonian University, Krakow, Poland

Abstract

Purpose/Aim—The goal of this study is to reveal how age-related changes in phospholipid (PL) composition in the fiber cell plasma membranes of the human eye lens affect the cholesterol (Chol) content at which Chol bilayer domains (CBDs) and Chol crystals start to form.

Materials and Methods—Saturation-recovery electron paramagnetic resonance with spin-labeled cholesterol analogs and differential scanning calorimetry were used to determine the Chol contents at which CBDs and cholesterol crystals, respectively, start to form in in membranes made of the major PL constituents of the plasma membrane of the human eye lens fiber cells. To preserve compositional homogeneity throughout the membrane suspension, the lipid multilamellar dispersions investigated in this work were prepared using a rapid solvent exchange method. The cholesterol content changed from 0 to 75 mol%.

Results—The saturation recovery electron paramagnetic resonance results show that CBDs start to form at 33, 50, 46, and 48 mol% Chol in the phosphatidylethanolamine, phosphatidylcholine, phosphatidylserine, and sphingomyelin bilayers, respectively. The differential scanning calorimetry results show that Chol crystals start to form at 50, 66, 70, and 66 mol% Chol in the phosphatidylethanolamine, phosphatidylcholine, phosphatidylserine, and sphingomyelin bilayers, respectively.

Conclusions—These results, as well those of our previous studies, indicate that the formation of CBDs precedes the formation of Chol crystals in all of the studied systems, and the appearance of each depends on the type of PL forming the bilayer. These findings contribute to a better understanding of the molecular mechanisms involved in the regulation of Chol-dependent processes in eye lens fiber cell membranes.

[*]Corresponding Author: Witold K. Subczynski, Department of Biophysics, Medical College of Wisconsin, 8701 Watertown Plank Road, Milwaukee, WI 53226, USA; Tel: (414) 955-4038; Fax: (414) 955-6512, subczyn@mcw.edu.
[⊥]Present address: Department of Physics, Boise State University, 1910 University Drive, Boise ID 83725, Tel: (208) 426-4003, laxmanmainali@boisestate.edu

Declaration of Interest
The authors report no conflicts of interest.

Author Manuscript Author Manuscript Author Manuscript Author Manuscript

Keywords

spin label; cholesterol saturation; cholesterol solubility threshold; lipid bilayer; eye lens

1. Introduction

The major function of the eye lens (together with the cornea) is to focus light on the retina, and to do this the lens must be transparent. In our opinion, three major features of the fiber cell plasma membrane of the human eye lens can affect the transparency: (1) drastic changes in the phospholipid (PL) composition that occur with age and are not observed in membranes of other tissues and organs [1–5]; (2) extremely high cholesterol (Chol) content, which also is not observed in membranes of other tissues and organs,[6–9] and (3) a lack of protein turnover and the lack of their transport from the old (nucleus) to the more recently synthetized (cortex) regions and *vice versa* [10,11]. These characteristics developed during biological evolution to perfect eye lens function.

The lack of the turnover of integral membrane proteins implies that the same proteins that performed certain functions just after their synthesis (during embryogenesis) should perform these same functions as the aging process takes place. However, this seemingly conflicts with the drastic changes in PL composition that occur during aging, which should affect the functioning of integral membrane proteins [12–15]. We investigated and discussed this issue in our previous works, which showed that the physical properties of the lipid bilayer of the eye lens membranes are independent of the changes in the PL composition, but only when the membranes are saturated with Chol.[16,17] Such a state is only possible when the membrane possesses a Chol reservoir in the form of pure cholesterol bilayer domains (CBDs) and is oversaturated with Chol. CBDs ensure Chol saturation of the lipid bilayer in which they are embedded and act as a buffer, releasing and incorporating Chol molecules [17,18].

The concept of the formation of the pure Chol bilayer immersed into Chol/PL membrane oversaturated with Chol was first proposed by Jacob et al. [19] based on small angle X-ray diffraction measurements of oriented multilamellar membrane samples. These measurements indicated the presence of Chol domains in the membrane with a unit cell periodicity of 34.0 Å. The same 34 Å pattern was observed in pseudo-bilayers of Chol in Chol crystals [20]. This suggested that in the Chol saturated multilamellar membrane, multiple closely associated ordered Chol layers were formed. Such a picture was not easily reconciled with packing of the thicker phospholipid bilayers but was consistent with phase separation into Chol crystals (for more discussion see [21]). Ziblat et al. [22] attempted to overcome this dilemma by exploring the molecular structure of single layers of lipid bilayers using grazing incidence X-ray diffraction. Diffraction from single bilayers was interpreted in terms of mixed layers of Chol/PLs, Chol as single bilayers, and Chol crystals. The experimental approach of that work and interpretation of the results are in accord with our investigations of CBDs. As was the case of our study, during sample preparation in Ref. [22] lipids were always in contact with water which protected the system from artefactual formation of Chol crystals. The film deposition method used in Ref. [19] faced this problem (see more discussion below and in Discussion section).

Author Manuscript Author Manuscript Author Manuscript Author Manuscript

Because the Chol saturation level can be different for each PL, the balance between the PL composition and Chol content in fiber cell membranes is important for the functioning of the membrane and the whole fiber cell, and for lens homeostasis [16,18]. This balance determines the conditions at which the PL bilayer is saturated with Chol. As discussed previously, to a large extent, CBDs ensure these conditions [17,18].

The relevant literature provides values for the cholesterol solubility thresholds (CSTs), i.e., the maximum amount of Chol accommodated in the PL bilayer, above which Chol precipitates in the form of crystals [23–28]. The data show that CSTs depend on the type of PL forming the bilayer [23,24,27,28]; however, for a given PL bilayer, the CST values indicated in the literature *vary*. This is mainly due to the way in which samples are prepared. Using the widely applied film deposition method, artefactual Chol crystals are formed as the chloroform solution of the Chol/PL mixture dries [23]. These crystals do not dissolve in the buffer rehydrating the mixture, and this crystalized fraction of Chol is not incorporated into the sample; in effect, the real Chol/PL molar ratio in the bilayer is smaller than the Chol/PL mixing ratio. The rapid solvent exchange method, which was applied in this study, is free from these shortcomings [23]. In some instances, the bilayer CST values prepared using these two methods differ significantly. For example, the CSTs for phosphatidylcholine (PC) bilayers established using the film deposition and rapid exchange methods are ~50 mol% [25] and ~66 mol% [23], respectively. An even larger discrepancy occurs for the phosphatidylserine (PS) bilayers for which the CSTs established using the two methods are ~33 mol% [27] and ~73 mol% [28], respectively. When the value of the Chol content is higher than that of the CST, Chol crystals are formed outside the bilayer.

The phase diagram published in our previous paper [21] shows the upper limits of Chol concentration (content) that can be accommodated within each phase of the dimyristoylphosphatidylcholine (DMPC) bilayer. At 27°C, the DMPC bilayer can accommodate ~6 mol% of Chol in the liquid-disordered phase (l_d). Above this concentration, a liquid-ordered phase (l_o) is formed with a Chol concentration of ~33 mol%. Thus, at Chol/PL mixing ratios from ~6 mol% up to ~33 mol%, both l_d and l_o phases coexist. At ~33 mol% Chol, the whole DMPC/Chol bilayer is in the liquid ordered phase, and at 50 mol% Chol, the DMPC bilayer is saturated with Chol; thus, 50 mol% Chol is the Chol saturation limit for the DMPC bilayer. Above this Chol concentration, excess Chol forms pure CBDs supported by the bulk membrane (DMPC saturated with Chol at ~50 mol %). Above 50 mol% Chol, the l_o phase becomes the structured l_o phase. The next limit, observed at ~66 mol% Chol, is the CST and specifies the total Chol content in the DMPC bilayer that can be dissolved in and supported by the bilayer (in the form of CBDs). Above this limit, a new phase is formed, namely Chol crystals.

In the present study, we evaluated the Chol saturation limits and CSTs for the bilayers comprising the major PL constituents of the fiber cell plasma membrane of the human eye lens, i.e., for PC, phosphatidylethanolamine (PE), PS, and sphingomyelin (SM). Because the major fatty acids in the fiber cell membranes of human eye lenses are palmitic (16:0, P) and oleic (18:1-*cis*, O) [4,6,7,29], we used PC, PE, PS with two acyl chains (POPC, POPE, POPS), and egg SM that contains 86% palmitoyl SM (PSM). The present results confirm that, similar to the DMPC bilayer [21], formation of CBDs precedes formation of Chol crystals in

Author Manuscript Author Manuscript Author Manuscript Author Manuscript

the POPC, POPE, POPS, and SM bilayers. Also, this study confirms that the values of the Chol saturation limits and CSTs depend on the types of PL forming the bilayer. These factors suggest that the balance between PL composition and Chol content in fiber cell membranes can regulate Chol-dependent processes in these membranes, and as a result, influence fiber cell and lens homeostasis.

2. Materials and Methods

2.1. Materials

PLs and Chol were purchased from Avanti Polar Lipids, Inc. (Alabaster, AL). They include one-palmitoy-2-oleoyl-*sn*-glycero-3-phosphatidylcholine (POPC), one-palmitoyl-2-oleoyl-sn-glycero-3-phosphoethanolamine (POPE), one-palmitoy-2-oleoyl-sn-glycero-3-phosphatidylserine (POPS), and egg sphingomyelin (SM). Spin labels, cholesterol analogue androstane spin label (ASL), and cholesterol analog cholestane spin label (CSL) were obtained from Molecular Probes (Eugene, OR). Other necessary chemicals (of at least reagent grade) were purchased from Sigma-Aldrich (St. Louis, MO).

2.2. Preparation of samples for EPR and DSC measurements

The Chol/PL membranes (dispersions of PLs and Chol in 10 mM PIPES and 150 mM NaCl, pH 7.0) were prepared using the rapid solvent exchange method [23,30,31]. The apparatus (described in detail in Ref. [31]) was built in our lab with the help of Dr. Jeffrey T. Buboltz (Univ Wisconsin Platteville, Platteville, WI, USA). For electron paramagnetic resonance (EPR) measurements, the membranes contained 1 mol% of spin labels added to the chloroform mixture of PL and Chol. To increase the signal-to-noise ratio, membrane suspensions were centrifuged for 15 min. at 12000 g and 4°C. The loose pellets, containing ~20% lipids (w/w), were put into a gas-permeable capillary, and EPR measurements were performed as described in Ref. [21]. Capillaries with a 0.6 mm i.d. and made from the gas permeable methylpentene polymer (TPX) were used. For differential scanning calorimetry (DSC) measurements, the membranes did not contain spin labels. To obtain a sample of the appropriate Chol/PL ratio for each investigated PL, the amount of cholesterol was kept constant (3 mg/mL for POPE and POPC, 10 mg/mL for SM and POPS), and the amount of PL was adjusted.

2.3. Saturation recovery EPR measurements

The T_1s of the spin labels were determined by analyzing the saturation recovery (SR) signal of the central line obtained by short-pulse SR EPR at X-band with the use of a loop-gap resonator [32,33]. The home-build SR spectrometer described previously in Ref. [34] (also see the review on SR by Hyde [35]) received two major hardware improvements. Now, the pump arm delivers a 1 W pulse to the loop-gap resonator. Also, the receiver dead time (after the saturating pump pulse) was decreased from 300 ns to 100 ns. These improvements were needed to detect and analyze SR signals containing fast components. To measure T_1s at different oxygen partial pressures (0% air, 30% air, or 50% air), the sample was equilibrated with the same gas that was used for temperature control (i.e., a controlled mixture of nitrogen and dry air adjusted with flow meters [Matheson Gas Products, model 7631H-604]) [36]. To measure the NiEDDA accessibility parameter, a 20 mM NiEDDA was present in the

Author Manuscript Author Manuscript Author Manuscript Author Manuscript

buffer, and samples were thoroughly deoxygenated [37]. All EPR measurements were performed at 37°C. Typically, 10^5–10^6 decays were acquired with 2048 data points on each decay. Sampling intervals were 4 ns, 5 ns, 10 ns, or 20 ns depending on oxygen tension. The total accumulation time was typically 2−5 min. SR signals were fitted by single- or double-exponential functions. When the single exponential fit was satisfactory, the decay time constant could be evaluated with a precision of ±3%. When the double exponential fit was necessary and satisfactory, the decay times were usually evaluated with a precision of ±12% and ±20% for longer and shorter recovery time constants, respectively. The presented work demonstrates that the use of relaxation agents (molecular oxygen or NiEDDA) is an excellent way to clearly discriminate and characterize two coexisting domains (phases) in lipid bilayers.

2.4. DSC measurements

DSC measurements were performed using a Nano DSC with platinum capillary cells obtained from TA Instruments, Inc. (Wood Dale, IL). The volume of the capillary cell of the instrument was 0.3 mL. The Nano DSCRun operating system software was used to acquire the data, and the NanoAnalyze software from TA instruments was used to analyze the data. All measurements were made at the constant scan rate of 1°C/min. The heat of transition of monohydrate Chol crystals (pure and contaminated by PLs) to anhydrous form was evaluated from the areas under the heating scan including all appropriate peaks and shoulders. The area under the heating scans was estimated using the integration baseline function (i.e., sigmoidal baseline) available on NanoAnalyze software. First, the integration region was selected. After that, pre- and post- baseline regions were adjusted to get the sigmoid curve baseline and the heat of transition was estimated. The precision of this evaluation was less than ±25%.

3. Results

3.1. Discrimination of CBDs

SR EPR spectroscopy was used to discriminate CBDs in the Chol/PL bilayers. Because the CBD is a pure Chol bilayer, it can only be discriminated from the surrounding bulk Chol-saturated PL bilayer by using Chol analog spin labels, ASL and CSL (see Fig. 1 for their structures), as discussed in our previous studies [37,38]. ASL, with a nitroxide moiety located close to the bilayer center, needs molecular oxygen for discrimination. The discrimination is possible because the local oxygen transport parameter in the CBD is much smaller than in the bulk bilayer [37,39]. Consequently, the oxygen-induced shortening of the relaxation time of ASL is also much smaller in the CBD than in the bulk bilayer. As a result, the SR signal of ASL can be fitted with two exponents, each arising from one of the two environments, the CBD and the bulk bilayer.

The opposite situation occurs in the case of CSL. The nitroxide moiety of CSL is located at the water/bilayer interface and is accessible to collisions with the water-soluble relaxation agent NiEDDA. This accessibility is significantly smaller when CSL is located in the bulk bilayer, because the PL polar head groups shield the nitroxide moiety, than when CSL is located in the CBD, where NiEDDA has practically free access to the CSL nitroxide moiety.

Author Manuscript Author Manuscript Author Manuscript Author Manuscript

Thus, the shortening of the relaxation time of CSL is much smaller in the bulk bilayer than in the CBD [37]. The double exponential SR signal indicates that, indeed, CSL is located in two environments, the CBD and the bulk bilayer.

Qualitatively discriminating SR EPR measurements were performed for the POPC, POPE, POPS, and SM bilayers. Their representative SR signals are presented in Fig. 2. When the Chol content is high enough (it can be different for different PLs), both ASL in the presence of molecular oxygen and CSL in the presence of the water-soluble relaxation agent NiEDDA indicate the existence of CBDs in all investigated membranes.

3.2. Discrimination of Chol crystals

DSC is a convenient method to indicate the formation of Chol crystals. To avoid the artefactual formation of the anhydrous Chol crystals, all preparations were made using the rapid solvent exchange method [21,23,30]. First, to better characterize the system, pure Chol samples were prepared using this method. In the absence of PLs, Chol formed only hydrated Chol crystals with the characteristic transition doublet peaks at 94°C and 96°C during the first heating scan, indicating a transition from the hydrated to anhydrous form (Fig. 3, scan 1). The ratio of the heights of the doublet peaks in hydrated Chol crystals changed with Chol concentration in the chloroform used for preparations. At a low Chol concentration, the broader peak at 94°C disappeared (Fig. 3, scan 2). When we used the film deposition method, we observed two characteristic peaks, one at ~40°C and the second at ~71°C (Fig. 3, scan 3). Based on the data from the literature we assigned the first peak to the transition between two different forms of anhydrous Chol crystals and the second peak to the transition of Chol crystals from the monohydrate to anhydrous form. In our preparations the buffer was added directly on the top of the film of dry Chol (to follow the same procedure in which liposomes were formed). In the basic paper [40] pure Chol was first dissolved in hot acetic acid and then the solution was allowed to slow cool to form anhydrous Chol crystals. On the first DSC heating scan, these crystals showed a transition between two different forms of anhydrous Chol crystals at 37°C. Monohydrate Chol crystals were obtained from recrystallization from 95% ethanol and they showed, on the first DSC heating scan, a transition from the monohydrated to anhydrous form at 86°C.

The first heating scans for suspensions of the POPC, POPE, POPS, and SM bilayers with different Chol contents are presented in Fig. 4. When Chol contents in the PL suspensions are above those of the CSTs, clear peaks are observed at 96°C, indicating the presence of Chol crystals in the suspensions. In the case of POPC (Fig. 4A) and SM (Fig. 4C), this peak is accompanied by a broad shoulder at lower temperatures. We think that peaks at 96°C are coming from pure Chol crystals, not contaminated by the presence of PLs. The broad shoulders are coming from Chol crystals containing PL impurities. Similar broad transitions of monohydrate Chol crystals to anhydrous form were observed earlier, when crystals were obtained in the presence of PLs [24,41]. In the case of PE (Fig. 4B), the additional peak observed at ~60°C indicates the transition of the PE bilayer from the lamellar to hexagonal phase [42]. This transition disappears when the Chol content is above ~50 mol%.

Author Manuscript Author Manuscript Author Manuscript Author Manuscript

3.3. Amount of Chol in CBDs

As explained in Sect. 3.1, when the Chol content in a Chol/PL bilayer is above the Chol saturation limit, the SR signal of the spin label in the presence of relaxation agents has two components: one from the spin label located in the CBD and one from the spin label located in the bulk bilayer. SR EPR is a solid qualitative method able to show the presence of CBDs in investigated membrane. The fractional contribution from the CBD to the SR signal should, in principle, provide clear-cut information about the amount of Chol associated with CBDs. However, this is true only in the case of spin labels with long spin-lattice relaxation times, when the pump power is really the saturating power (see Ref. [43] for more explanations). Relaxation agents (molecular oxygen and NiEDDA) significantly shorten T_{1s} making it impossible to saturate the SR signals. Because of that, the contribution of each component to the SR signal is not a robust parameter providing information about the amount of Chol associated with CBDs, but it is assumed to be proportional to the amount of Chol giving the particular signal. Here, the relative content of Chol in CBDs is specified by the normalized pre-exponential coefficients obtained from fitting a double exponential function to the experimental SR signals. This evaluation can be performed for bilayers with different Chol/PL molar ratios. The results for both Chol analogs in each the POPC, POPE, POPS, and SM bilayers were used to construct Fig. 5. It should be noted that the results contain information about the amount of Chol in all CBDs, not in individual CBDs.

3.4. Amount of Chol in Chol crystals

Fig. 4 qualitatively illustrates that the range of the Chol contents at which Chol crystals form in membrane suspensions depends on the type of PL forming these membranes. The excess enthalpy values obtained from the areas under the heating scans, including the peak at 96°C and the shoulder (see Sect. 2.4), are proportional to the amount of Chol associated with all forms of Chol crystals produced in the PL suspensions. Fig. 5 was constructed using the amount of Chol in Chol crystals for a given sample determined from the area under the heating scans.

3.5. Chol content at which CBDs and Chol crystals start to form

Our final goal was to use the SR and DSC measurements to evaluate the Chol contents at which CBDs and Chol crystals start to form in the PC, PE, PS, and SM bilayers. To do this, we plotted the values of the Chol contents in CBDs and Chol crystals as a function of the Chol/PL mixing ratio; see Fig. 5. Extrapolating the data obtained at different Chol/PL mixing ratios to the “zero” amount of Chol in CBDs or in Chol crystals gives the Chol content value (mixing ratio) at which these structures begin to form. These procedures for the POPC, POPE, POPS, and SM bilayers are presented in Fig. 5, and the evaluated values of Chol contents at which CBDs and Chol crystals start to form are presented in Table 1.

4. Discussion

During aging, the PL composition of the fiber cells plasma membranes of the human eye lens changes drastically [1,5]. In mature fiber cells, about 2/3 (66%) of PLs are SMs and ~80% of them are dihydro-SMs [29]. In young cells, SM constitutes only ~33 mol% of PLs [1,4]. These drastic, age-related changes in lipid composition certainly impair homeostasis of the

Author Manuscript Author Manuscript Author Manuscript Author Manuscript

fiber cell membranes and lens as a whole. Thus, it is no surprise that during evolution, a special mechanism was designed to counteract this impairment. We suppose that this mechanism involves permanent saturation of the fiber cell membranes with Chol which ensure that the physical properties of the membrane do not change with the PL composition [16,17,44,45]. To ensure saturation with Chol, fiber cell plasma membranes have to be oversaturated with Chol to the level that pure CBDs are present, because CBDs provide the buffering capacities for Chol in the surrounding PL bilayer, ensuring its saturation with Chol [18].

In this study, we evaluated the Chol contents at which CBDs and Chol crystals start to form in bilayers comprising the major PLs of the fiber cell plasma membrane, i.e., POPE, POPC, POPS, and SM (Table 1). The values of the CSTs (Table 1) are in line with data from the literature [23,24,28], and indicate that the CSTs are different for different PLs. To the best of our knowledge the first evaluation of the Chol content at which CBDs start to form in PL bilayers was attempted by Ziblat et al. [22]. The value which they obtained for the DPPC bilayer is very close to that obtained by us in the present work for the POPC bilayer and earlier for the DMPC bilayer [21]. Small differences in the values of Chol content arise probably from different temperatures at which experiments were performed, 7°C in Ref. [22] and 37°C in this study. Moreover, in Ziblat et al. [22], the DPPC-Chol bilayer contained an additional 10 mol% of POPC. A greater difference in the values of Chol content in the case of the SM bilayers can be explained by differences in the interpretation of the results by us and by Ziblat et al. [22] (see the paragraph below). When evaluating the Chol saturation limits both groups determined the Chol content at which CBDs start to form by extrapolation of the intensity of the signals coming from CBDs to zero.

We would like to stress that when investigating bilayers saturated and oversaturated with Chol, the manner in which the liposomes are prepared is crucial. As discussed in the Introduction section, when the film deposition method is used, artefactual Chol crystals form as the chloroform solution of the Chol/PL mixtures dries (see also Fig. 3). To avoid this, we prepared the liposomes using the rapid solvent exchange method. Use of this method revealed that the formation of CBDs precedes formation of Chol crystals in all the investigated Chol/PL bilayers. Also, this method showed that the Chol contents at which CBDs and Chol crystals start to form are very similar for the POPC, POPS, and SM bilayers but differ significantly from that of the POPE bilayer (Table 1). This difference might result from different ability of PL head groups to interact with one another at the bilayer/water interface. Whereas the POPC bilayer has only hydrogen bond (H-bond) acceptor groups, the POPS, POPE, and SM bilayers have both H-bond donor and acceptor groups, so they are potentially able to make inter-lipid H-bonds at the bilayer/water interface. However, POPS has a net negative electrostatic charge, so the POPS head groups repel one another and H-bonds practically do not form. Thus, both the POPS and POPC bilayers can accommodate a significant amount of Chol before it becomes saturated with Chol. The H-bonds donor groups of a SM molecule are below the phosphate group, so they are not easily accessible to acceptor groups of other SM molecules and inter-lipid H-bonds are not frequent in contrast to SM-Chol H-bonds that are numerous [46]. Thus, Chol can accommodate easily in the SM bilayer. PE has an amine group that forms strong hydrogen bonds with the neighboring phosphate groups; besides, the PE head group has a smaller size than those of the other three

Author Manuscript Author Manuscript Author Manuscript Author Manuscript

phospholipids [47] so packing of lipids in this bilayer is dense and the bilayer is not able to accommodate as much Chol as the other bilayers. These differences in the abilities of Chol accommodation give a certain “freedom” to the organism to regulate the amount of membrane Chol at which CBDs and Chol crystals form, by using mixtures of these PLs. For fiber cell plasma membranes in the human eye lens, the apparent tendency is that as an individual gets older, CBDs and, in particular, Chol crystals begin forming at higher Chol contents; this is due to the increase in the proportion of SM/PE in the membrane.

Assuming that the Chol content values at which CBDs and Chol crystals start to form in PL mixtures are the weighted sums of the individual Chol content values for each PL, with the weight equal to the mol% of the PL in the mixture, a phase diagram can be created as shown in Fig. 6. This diagram indicates the regions in which CBDs are embedded into the surrounding mixed PL bilayer saturated with Chol and forming a structured [48] (or dispersed [49]) liquid ordered phase. The reasons why the CBD cannot be considered as a separate phase is discussed in detail in Ref. [21] This diagram also shows the region in which Chol crystals (which now form a new phase) coexist with the structured liquid ordered phase. This phase diagram clearly shows boundaries and their dependences on PL compositions. For fiber cell plasma membranes of the human eye lens, only one PL, namely PE, can decrease the Chol content at which CBDs and Chol crystals start to form. The literature data shows that the amount of PE in fiber cell membranes decreases with age and in the deeper located fiber cell layers[1,4]. As a result, the proportion of SM/PE increases, shifting formation of CBDs and Chol crystals to higher Chol contents. Data from this new investigation, as well as previously published data [21], indicate that the balance between the PL composition and the Chol content forms a mechanism of regulation for Chol-dependent processes in fiber cell plasma membranes of the human eye lens, and this mechanism has yet to be investigated in detail.

The presented phase diagram (Fig. 6) is valid for PLs with saturated acyl chains or with one mono-*cis*-unsaturated chain. Data from the literature [50,51] and our own observations [52] indicate that the presence of polyunsaturated acyl chains in PLs, as well as the peroxidation of these chains, decreases the Chol content at which CBDs and Chol crystals start to form. These dependences are schematically illustrated in Fig. 7 and can be used as the universal guideline for investigations of Chol-dependent processes in membranes with different PL compositions, different degrees of acyl chain unsaturation, and under different levels of oxidative stress.

5. Conclusions

In this study, we demonstrated that the formation of CBDs precedes the formation of Chol crystals in membranes comprising the major PLs of the fiber cell plasma membrane of the human eye lens, including glycerophospholipids and sphingolipids. We believe this finding is also valid for other PL membranes loaded and overloaded with Chol. We also demonstrated that the Chol contents at which CBDs and Chol crystals start to form depend on the type of PL forming the bulk bilayer. Based on these findings, we proposed a phase diagram for mixtures of PLs and Chol that indicates the phase boundaries and regions of PL and Chol concentrations at which CBDs and Chol crystals are formed. In the Discussion, we

Author Manuscript Author Manuscript Author Manuscript Author Manuscript

also indicated that factors such as polyunsaturation and peroxidation of PL acyl chains can strongly decrease the Chol contents at which CBDs and Chol crystals start to form. All these findings contribute to a better understanding of the molecular mechanisms that are involved in the regulation of Chol-dependent processes in membranes.

Acknowledgments

Research reported in this publication was supported by the National Institutes of Health (USA) under Grants R01 EY015526, P41 EB001980, and P30 EY001931 and by the Polish National Science Center under Grant 2016/22/M/NZ1/0187.

REFERENCES

1. Huang L, Grami V, Marrero Y, Tang D, Yappert MC, Rasi V, Borchman D. Human lens phospholipid changes with age and cataract. Invest Ophthalmol Vis Sci 2005;46:1682–1689. [PubMed: 15851569]
2. Paterson CA, Zeng J, Husseini Z, Borchman D, Delamere NA, Garland D, Jimenez-Asensio J. Calcium ATPase activity and membrane structure in clear and cataractous human lenses. Curr Eye Res 1997;16:333–338. [PubMed: 9134322]
3. Truscott RJ. Age-related nuclear cataract: a lens transport problem. Ophthalmic Res 2000;32:185–194. [PubMed: 10971179]
4. Yappert MC, Rujoi M, Borchman D, Vorobyov I, Estrada R. Glycero- versus sphingo-phospholipids: correlations with human and non-human mammalian lens growth. Exp Eye Res 2003;76:725–734. [PubMed: 12742355]
5. Hughes JR, Deeley JM, Blanksby SJ, Leisch F, Ellis SR, Truscott RJ, Mitchell TW. Instability of the cellular lipidome with age. Age 2012;34:935–947. [PubMed: 21894448]
6. Li LK, So L, Spector A. Membrane cholesterol and phospholipid in consecutive concentric sections of human lenses. J Lipid Res 1985;26:600–609. [PubMed: 4020298]
7. Li LK, So L, Spector A. Age-dependent changes in the distribution and concentration of human lens cholesterol and phospholipids. Biochim Biophys Acta 1987;917:112–120. [PubMed: 3790601]
8. Rujoi M, Jin J, Borchman D, Tang D, Yappert MC. Isolation and lipid characterization of cholesterol-enriched fractions in cortical and nuclear human lens fibers. Invest Ophthalmol Vis Sci 2003;44:1634–1642. [PubMed: 12657603]
9. Zelenka PS. Lens lipids. Curr Eye Res 1984;3:1337–1359. [PubMed: 6391828]
10. Lynnerup N, Kjeldsen H, Heegaard S, Jacobsen C, Heinemeier J. Radiocarbon dating of the human eye lens crystallines reveal proteins without carbon turnover throughout life. PloS One 2008;3:e1529. [PubMed: 18231610]
11. Stewart DN, Lango J, Nambiar KP, Falso MJ, FitzGerald PG, Rocke DM, Hammock BD, Buchholz BA. Carbon turnover in the water-soluble protein of the adult human lens. Mol Vis 2013;19:463–475. [PubMed: 23441119]
12. Epand RM. Role of membrane lipids in modulating the activity of membrane-bound enzymes In: Yeagle PL, editor. The Structure of Biological Membrane. Boca Raton: CRC Press; 2005 pp 499–509.
13. Reichow SL, Gonen T. Lipid-protein interactions probed by electron crystallography. Curr Opin Struct Biol 2009;19:560–565. [PubMed: 19679462]
14. Tong J, Briggs Margaret M, McIntosh Thomas J. Water permeability of aquaporin-4 channel depends on bilayer composition, thickness, and elasticity. Biophys J 2012;103:1899–1908. [PubMed: 23199918]
15. Tong J, Canty JT, Briggs MM, McIntosh TJ. The water permeability of lens aquaporin-0 depends on its lipid bilayer environment. Exp Eye Res 2013;113:32–40. [PubMed: 23680159]
16. Mainali L, Raguz M, O'Brien WJ, Subczynski WK. Changes in the properties and organization of human lens lipid membranes occurring with age. Curr Eye Res 2017;42:721–731. [PubMed: 27791387]

Author Manuscript Author Manuscript Author Manuscript Author Manuscript

17. Subczynski WK, Raguz M, Widomska J, Mainali L, Konovalov A. Functions of cholesterol and the cholesterol bilayer domain specific to the fiber-cell plasma membrane of the eye lens. J Membr Biol 2012;245:51–68. [PubMed: 22207480]
18. Subczynski WK, Mainali L, Raguz M, O'Brien WJ. Organization of lipids in fiber-cell plasma membranes of the eye lens. Exp Eye Res 2017;156:79–86. [PubMed: 26988627]
19. Jacob RF, Cenedella RJ, Mason RP. Direct evidence for immiscible cholesterol domains in human ocular lens fiber cell plasma membranes. J Biol Chem 1999;274:31613–31618. [PubMed: 10531368]
20. Huang J, Buboltz JT, Feigenson GW. Maximum solubility of cholesterol in phosphatidylcholine and phosphatidylethanolamine bilayers. Biochim Biophys Acta 1999;1417:89–100. [PubMed: 10076038]
21. Mainali L, Raguz M, Subczynski WK. Formation of cholesterol bilayer domains precedes formation of cholesterol Crystals in cholesterol/dimyristoylphosphatidylcholine membranes: EPR and DSC studies. J Phys Chem B 2013;117:8994–9003. [PubMed: 23834375]
22. Ziblat R, Leiserowitz L, Addadi L. Crystalline domain structure and cholesterol crystal nucleation in single hydrated DPPC:cholesterol:POPC bilayers. J Am Chem Soc 2010;132:9920–9927. [PubMed: 20586463]
23. Huang J, Buboltz JT, Feigenson GW. Maximum solubility of cholesterol in phosphatidylcholine and phosphatidylethanolamine bilayers. Biochim Biophys Acta 1999;1417:89–100. [PubMed: 10076038]
24. Epand RM. Cholesterol in bilayers of sphingomyelin or dihydrosphingomyelin at concentrations found in ocular lens membranes. Biophys J 2003;84:3102–3110. [PubMed: 12719240]
25. Epand RM, Bain AD, Sayer BG, Bach D, Wachtel E. Properties of mixtures of cholesterol with phosphatidylcholine or with phosphatidylserine studied by (13)C magic angle spinning nuclear magnetic resonance. Biophys J 2002;83:2053–2063. [PubMed: 12324423]
26. Benatti CR, Lamy MT, Epand RM. Cationic amphiphiles and the solubilization of cholesterol crystallites in membrane bilayers. Biochim Biophys Acta 2008;1778:844–853. [PubMed: 18201547]
27. Bach D, Wachtel E, Borochov N, Senisterra G, Epand RM. Phase behaviour of heteroacid phosphatidylserines and cholesterol. Chem Phys Lipids 1992;63:105–113.
28. Garg S, Castro-Roman F, Porcar L, Butler P, Bautista PJ, Krzyzanowski N, Perez-Salas U. Cholesterol solubility limit in lipid membranes probed by small angle neutron scattering and MD simulations. Soft Matter 2014;10:9313–9317. [PubMed: 25338228]
29. Deeley JM, Mitchell TW, Wei X, Korth J, Nealon JR, Blanksby SJ, Truscott RJ. Human lens lipids differ markedly from those of commonly used experimental animals. Biochim Biophys Acta 2008;1781:288–298. [PubMed: 18474264]
30. Buboltz JT, Feigenson GW. A novel strategy for the preparation of liposomes: rapid solvent exchange. Biochim Biophys Acta 1999;1417:232–245. [PubMed: 10082799]
31. Buboltz JT. A more efficient device for preparing model-membrane liposomes by the rapid solvent exchange method. Rev Sci Instrum 2009;80:124301. [PubMed: 20059155]
32. Yin JJ, Feix JB, Hyde JS. Mapping of collision frequencies for stearic acid spin labels by saturation-recovery electron paramagnetic resonance. Biophys J 1990;58:713–720. [PubMed: 2169919]
33. Yin JJ, Pasenkiewicz-Gierula M, Hyde JS. Lateral diffusion of lipids in membranes by pulse saturation recovery electron spin resonance. Proc Natl Acad Sci U S A 1987;84:964–968. [PubMed: 3029766]
34. Mainali L, Camenisch TG, Hyde JS, Subczynski WK. Saturation recovery EPR spin-labeling method for quantification of lipids in biological membrane domains. Appl Magn Reson 2017;48:1355–1373. [PubMed: 29805201]
35. Hyde JS. Saturation recovery In Foundations of Modern EPR. Eaton GR, Eaton SS, and Salikhov KM, editors. World Scientific, Singapore 1998 pp 607–618.
36. Subczynski WK, Felix CC, Klug CS, Hyde JS. Concentration by centrifugation for gas exchange EPR oximetry measurements with loop-gap resonators. J Magn Reson 2005;176:244–248. [PubMed: 16040261]

Author Manuscript Author Manuscript Author Manuscript Author Manuscript

37. Raguz M, Mainali L, Widomska J, Subczynski WK. Using spin-label electron paramagnetic resonance (EPR) to discriminate and characterize the cholesterol bilayer domain. Chem Phys Lipids 2011;164:819–829. [PubMed: 21855534]
38. Subczynski WK, Raguz M, Widomska J. Studying lipid organization in biological membranes using liposomes and EPR spin labeling. Methods Mol Biol 2010;606:247–269. [PubMed: 20013402]
39. Plesnar E, Szczelina R, Subczynski WK, Pasenkiewicz-Gierula M. Is the cholesterol bilayer domain a barrier to oxygen transport into the eye lens? Biochim Biophys Acta 2018;1860:434–441.
40. Loomis CR, Shipley GG, Small DM. The phase behavior of hydrated cholesterol. J Lipid Res 1979;20:525–535. [PubMed: 458269]
41. Epand RM, Hughes DW, Sayer BG, Borochov N, Bach D, Wachtel E. Novel properties of cholesterol-dioleoylphosphatidylcholine mixtures. Biochim Biophys Acta 2003;1616:196–208. [PubMed: 14561477]
42. Paré C, Lafleur M. Polymorphism of POPE/Cholesterol System: A 2H Nuclear magnetic resonance and infrared spectroscopic investigation. Biophys J 1998;74:899–909. [PubMed: 9533701]
43. Mainali L, Camenisch TG, Hyde JS, Subczynski WK. Saturation recovery EPR spin-labeling method for quantification of lipids in biological membrane domains. Appl Magn Reson 2017;48:1355–1373. [PubMed: 29805201]
44. Mainali L, Raguz M, O'Brien WJ, Subczynski WK. Properties of membranes derived from the total lipids extracted from the human lens cortex and nucleus. Biochim Biophys Acta 2013;1828:1432–1440. [PubMed: 23438364]
45. Mainali L, Raguz M, O'Brien WJ, Subczynski WK. Properties of membranes derived from the total lipids extracted from clear and cataractous lenses of 61–70-year-old human donors. Eur Biophys J 2015;44:91–102. [PubMed: 25502634]
46. Rog T, Pasenkiewicz-Gierula M. Cholesterol-sphingomyelin interactions: a molecular dynamics simulation study. Biophys J 2006;91:3756–3767. [PubMed: 16920840]
47. Suits B, Pitman MC, Feller SE. Molecular dynamics investigation of the structural properties of phosphatidylethanolamine lipid bilayers. J Chem Phys 2005;122:244714. [PubMed: 16035800]
48. Heberle FA, Feigenson GW. Phase separation in lipid membranes. Cold Spring Harb Perspect Biol 2011;3:1–13.
49. Simons K, Vaz WL. Model systems, lipid rafts, and cell membranes. Rev Biophys Biomol Struct 2004;33:269–295.
50. Jacob RF, Mason RP. Lipid peroxidation induces cholesterol domain formation in model membranes. J Biol Chem 2005;280:39380–39387. [PubMed: 16195227]
51. Jacob RF, Aleo MD, Self-Medlin Y, Doshna CM, Mason RP. 1,2-naphthoquinone stimulates lipid peroxidation and cholesterol domain formation in model membranes. Invest Ophthalmol Vis Sci 2013;54:7189–7197. [PubMed: 24130176]
52. Mainali L, Zareba M, Subczynski WK. Oxidation of polyunsaturated phospholipid decreases the cholesterol content at which cholesterol bilayer domains start to form in phospholipid-cholesterol membranes. Biophys J 2017;112:375a.

Author Manuscript Author Manuscript Author Manuscript Author Manuscript

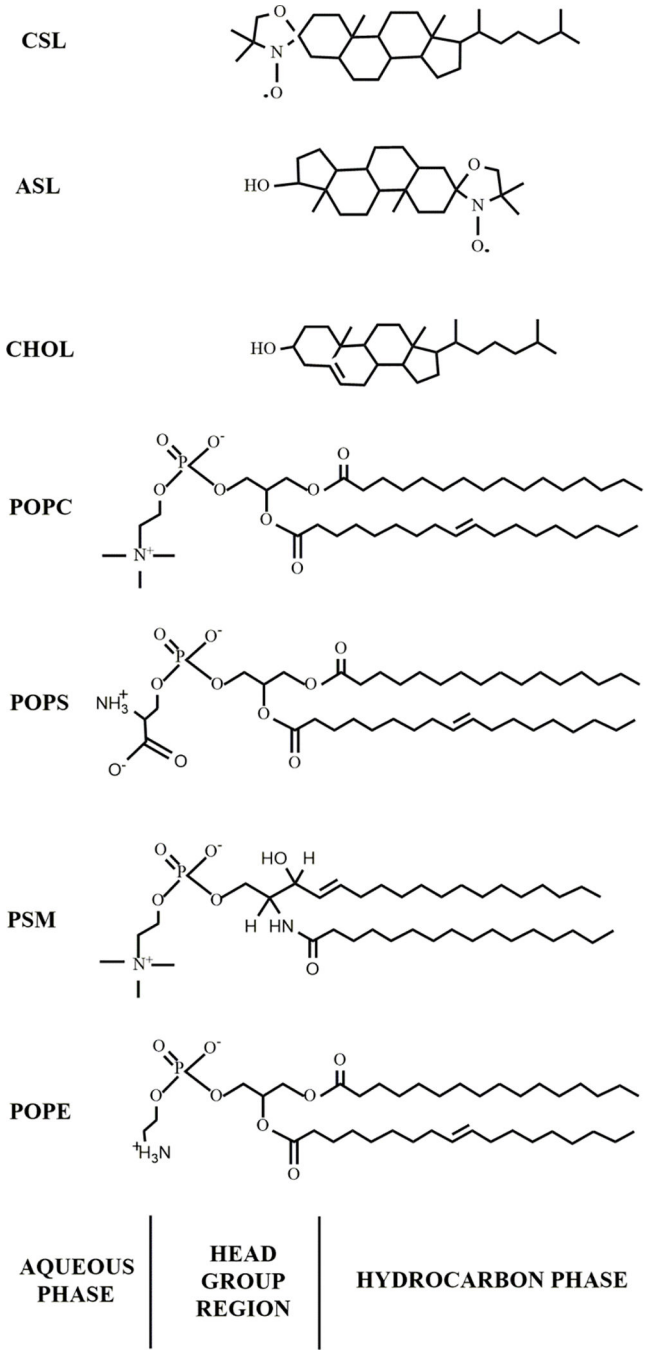

Figure 1.

Chemical structures of Chol analog spin labels used in this work: ASL and CSL. Chemical structures of four major PLs of fiber cell plasma membranes of the human eye lens. POPC, POPS, PSM, and POPE were used in the presented investigation. These structures indicate the approximate locations of the molecules and Chol analogs across the PL bilayer membrane. We used egg SM, a natural phospholipid that contains 86% palmitoyl SM (PSM).

Author Manuscript
Author Manuscript
Author Manuscript
Author Manuscript

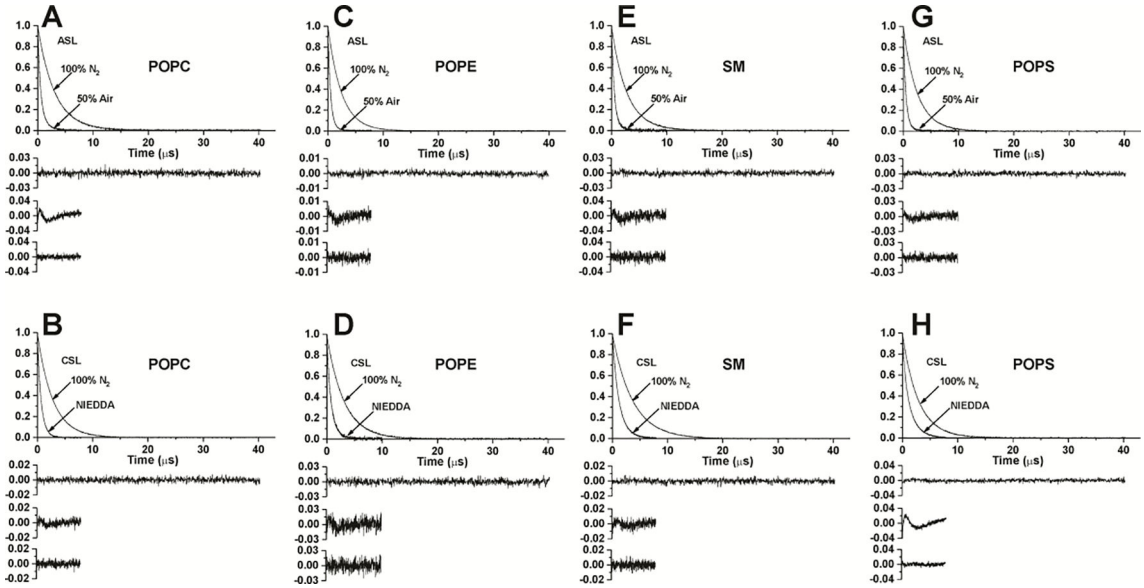

Figure 2.

Representative SR signals with fitted curves and residuals (the experimental signal minus the fitted curve) for ASL (A, C, E, G) and CSL (B, D, F, H) in Chol/POPC membranes with a Chol/POPC mixing ratio of 1.5 (A, B), Chol/POPE membranes with a Chol/POPE mixing ratio of 0.65 (C, D), Chol/SM membranes with a Chol/SM mixing ratio of 1.25 (E, F), and Chol/POPS membranes with a Chol/POPS mixing ratio of 1.25 (G, H). Signals were recorded at 37°C for samples equilibrated with 100% nitrogen, with a gas mixture of 50% air and 50% nitrogen (A, C, E, G) and in the presence of NiEDDA (B, D, F, H). SR signals were satisfactorily fitted to a single-exponential function in the absence of molecular oxygen with time constants of 3.05 ± 0.004 μs (A), 2.42 ± 0.001 μs (C), 2.76 ± 0.003 μs (E), 2.53 ± 0.003 μs (G), 2.74 ± 0.003 μs (B), 3.07 ± 0.005 μs (D), 3.64 ± 0.003 μs (F), 2.86 ± 0.003 μs (H) (the upper residuals are for a single-exponential fit). SR signals in the presence of molecular oxygen can be fitted satisfactorily with a double-exponential curve for ASL with time constants of 1.09 ± 0.02 μs and 0.43 ± 0.006 μs (A), 0.77 ± 0.06 μs and 0.44 ± 0.005 μs (C), 1.11 ± 0.12 μs and 0.45 ± 0.01 μs (E), 1.06 ± 0.11 μs and 0.44 ± 0.006 μs (G) (middle residuals are for single-exponential fits and lower residuals are for double-exponential fits). SRs signal in the presence of NiEDDA can be fitted satisfactorily with a double-exponential curve for CSL with time constants of 0.79 ± 0.03 μs and 0.53 ± 0.03 μs (B), 0.92 ± 0.02 μs and 0.42 ± 0.04 μs (D), 1.34 ± 0.04 μs and 0.80 ± 0.07 μs (F), 1.49 ± 0.007 μs and 0.40 ± 0.006 μs (H) (middle residuals are for single-exponential fits and lower residuals are for double-exponential fits).

Author Manuscript Author Manuscript Author Manuscript Author Manuscript

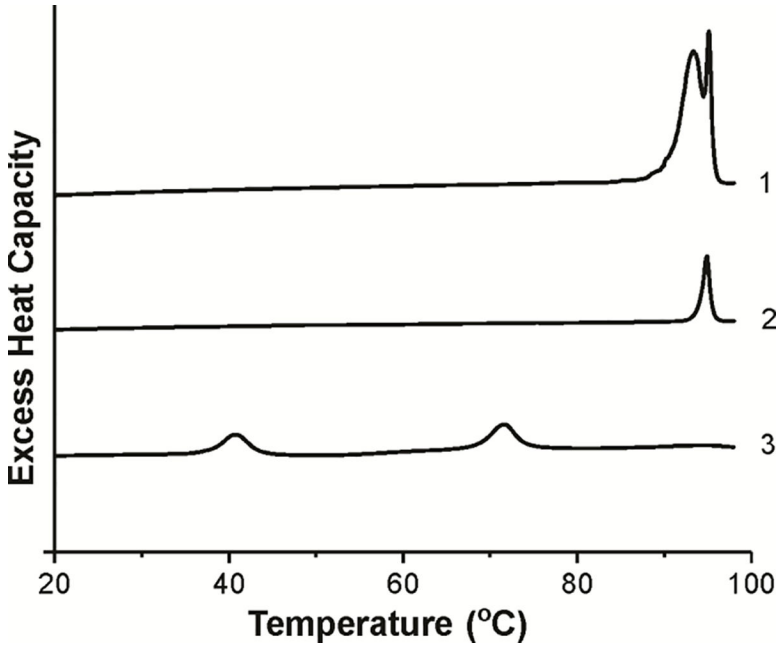

Figure 3.

The first DSC heating scans of the dispersion of Chol crystals prepared using the rapid solvent exchange method (scans 1 and 2) and the film deposition method (scan 3). The concentration of Chol in chloroform was 25 mg/ml (scan 1) and 1 mg/ml (scan 2).

Author Manuscript Author Manuscript Author Manuscript Author Manuscript

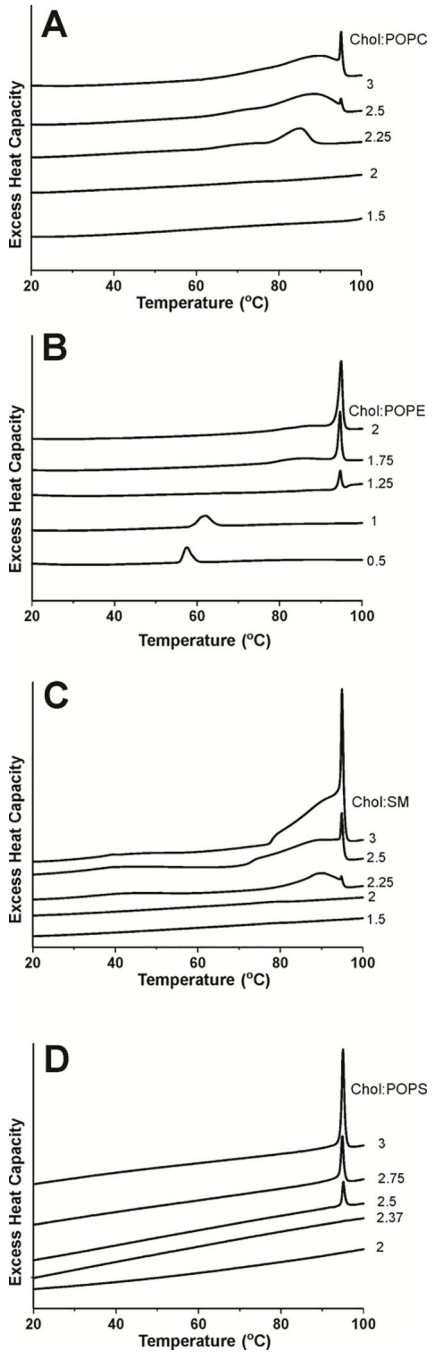

Figure 4.
The first DSC heating scans of Chol/PL dispersions with different Chol contents.

Author Manuscript Author Manuscript Author Manuscript Author Manuscript

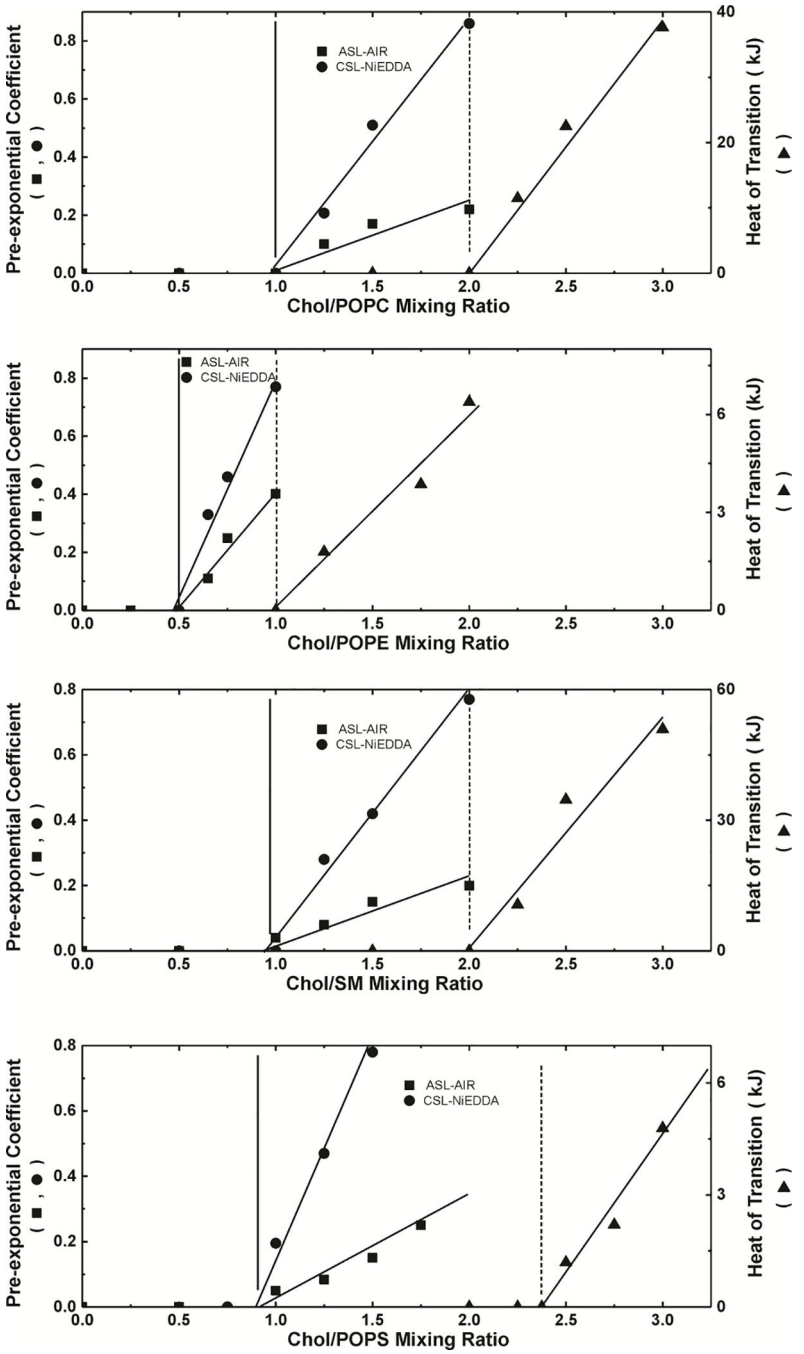

Figure 5.

Plot of the pre-exponential coefficient of the CBD component in the SR signal obtained from measurements with ASL (■) and CSL (●), and the excess enthalpy value (area under the peak) at ~96°C plotted as a function of cholesterol content (Chol/PL molar ratio) (▲) in PL suspension. Pre-exponential coefficients were measured for samples equilibrated with 50% air (ASL) and in the presence of 20 mM NiEDDA (CSL). Vertical solid and broken lines indicate the Chol saturation limit and the CST in the PL membrane.

Author Manuscript Author Manuscript Author Manuscript Author Manuscript

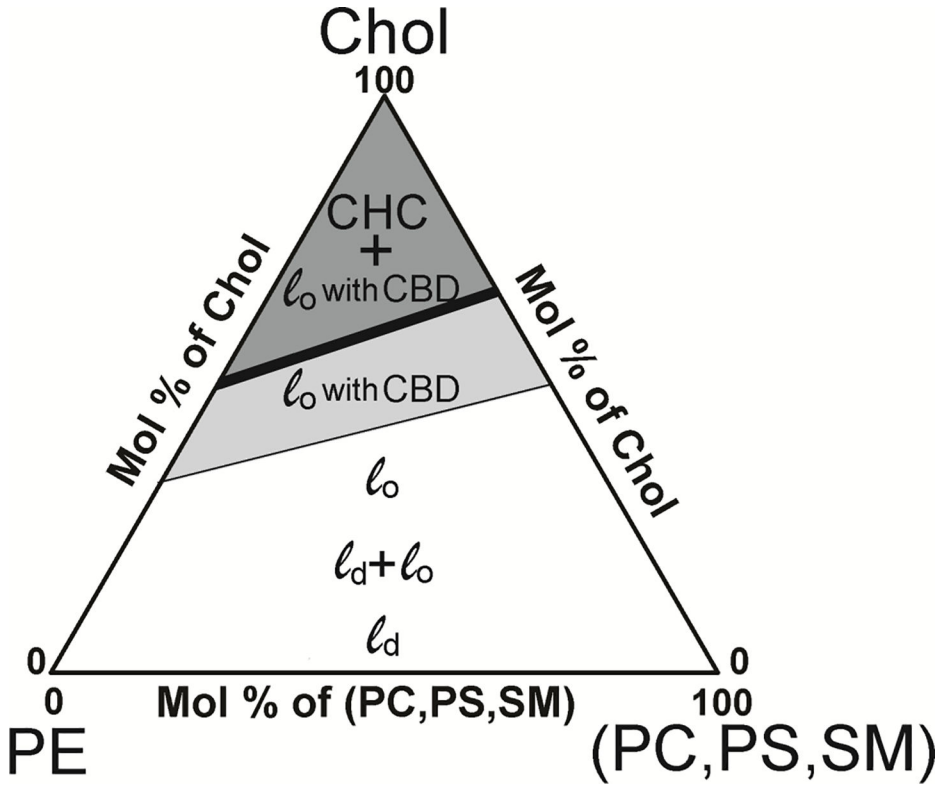

Figure 6.

Hypothetical fluid phase diagram for mixtures of the most abundant lens PLs (PS, PC, PE, and SM) and Chol. It is assumed that the Chol saturation limit (thin line) and the CST (thick line) for the phospholipid mixture are the weighted sums of the Chol saturation limits and CSTs for individual PLs with a weight equal to the mole fraction of the individual PLs in the mixture. The white area indicates the portion of the phase diagram where PL bilayers can accommodate Chol, forming the liquid disordered (l_d) phase, coexisting liquid disordered and liquid ordered ($l_d + l_o$) phases, and the liquid ordered (l_o) phase. At Chol contents greater than the Chol saturation limit (light gray area), CBDs start to form, and the liquid ordered phase becomes a structured liquid ordered phase. At Chol contents greater than the CST (dark gray area), a new phase, namely Chol crystals (CHCs) are formed in equilibrium with the structured liquid ordered phase. The phase diagram presented here differs significantly from the hypothetical phase diagram we presented eight years ago [18]. The previous one was based only on the literature CST data obtained mainly for liposomes prepared using the film deposition method with artefactual Chol crystals formed during preparation (see the Introduction for more explanation). Also, at that time the data were not yet available to indicate Chol contents at which CBDs start to form.

Author Manuscript Author Manuscript Author Manuscript Author Manuscript

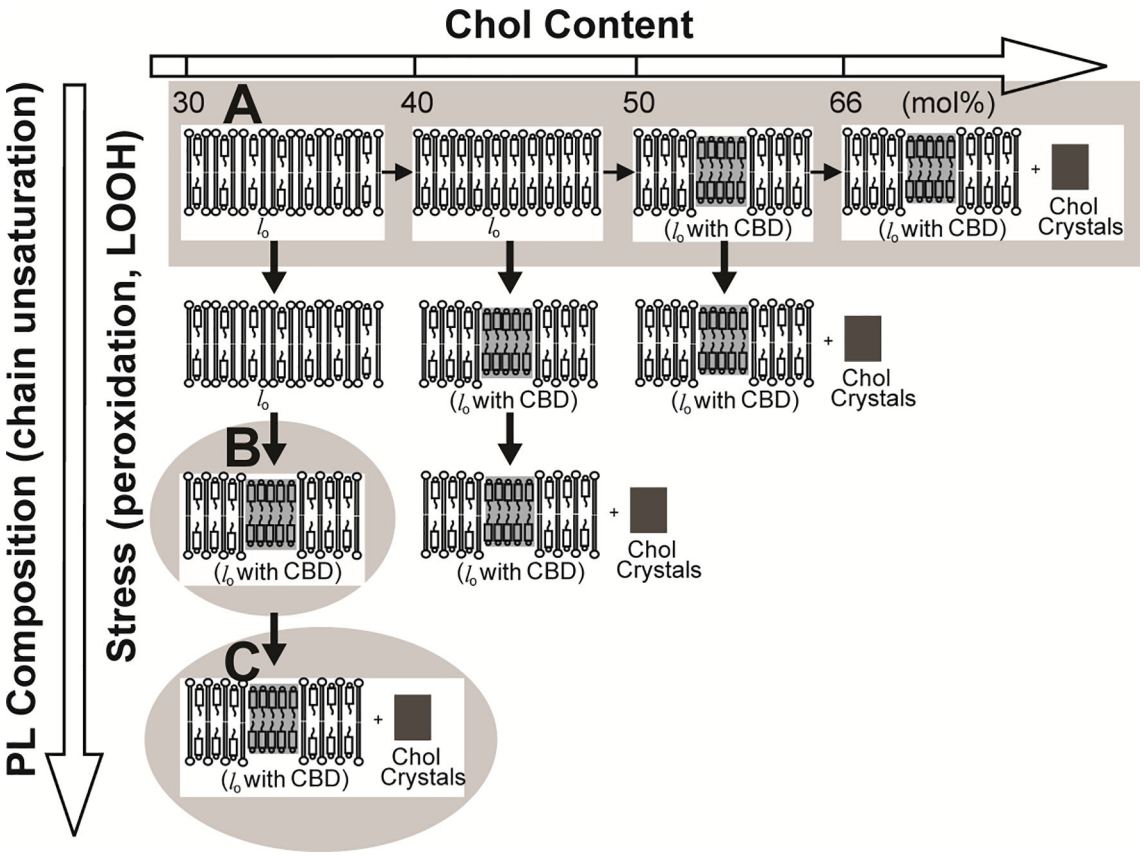

Figure 7.

Hypothetical pathways leading to the formation of CBDs and Chol crystals. Factors decreasing the Chol content at which CBDs and Chol crystals start to form are indicated. In saturated PC membranes (and in monounsaturated models of human eye lens lipid membranes), CBDs were observed at Chol contents exceeding ~50 mol%, and Chol crystals started to form at ~66 mol% Chol (A). In the freshly formed polyunsaturated membranes (made of dilinoleoylphosphatidylcholine), CBDs were observed at ~37 mol% (B). After three days of autoxidation, Chol crystals, in addition to CBDs, were formed in this membrane suspension (C).

Author Manuscript

Author Manuscript

Author Manuscript

Author Manuscript

Table 1.

Chol contents at which CBDs (Chol saturation limit) and Chol crystals (CST) start to form

Phospholipid	Chol saturation limit (mol%)	CST (mol%)
POPE	33	50
POPC	50	66
POPS	46	70
SM	48	66